

Assembly and Processing of Hydrogen Bond Induced Supramolecular Nanostructures

D. L. Keeling,[†] N. S. Oxtoby,[‡] C. Wilson,[‡] M. J. Humphry,[†]
N. R. Champness,^{*,†} and P. H. Beton^{*,†}

*Schools of Physics & Astronomy and Chemistry, University of Nottingham,
Nottingham NG7 2RD, UK*

Received September 27, 2002

ABSTRACT

The adsorption of a diimide derivative (NTCDI) of naphthalene tetracarboxylic dianhydride (NTCDA) on the Ag/Si(111)- $\sqrt{3} \times \sqrt{3}R30^\circ$ surface has been investigated using ultrahigh vacuum (UHV) scanning tunneling microscopy (STM). Hydrogen bonding, mediated by the imide groups, controls the ordering of adsorbed molecules, resulting in extended rows up to 20 nm in length with an intermolecular separation of 1.5 lattice constants. A near-identical row motif is observed in the molecular packing of crystalline NTCDI. Tip-adsorbate interactions lead to modification and repositioning of supramolecular nanostructures.

The self-assembly of supramolecular structures is governed by directional, selective, noncovalent interactions between neighboring molecules. These interactions result from the incorporation of functional groups that give rise to, for example, hydrogen-bonding or metal coordination, and act to order spontaneously an ensemble of molecules into larger and more complex structures. Supramolecular assembly of soluble precursor molecules in the solution phase to afford either discrete molecular architectures or to construct crystalline polymeric arrays is now a well-established area of research, and many complex materials have been synthesized using this approach.¹ However, the use of similar intermolecular interactions to control assembly on surfaces represents a much newer field of research, with the first demonstrations published only in the past few years. In particular, hydrogen-bonding and dipole–dipole interactions have been exploited to form rows and molecular aggregates including dimers, trimers, tetramers, and decamers.^{2–6}

A particularly exciting aspect of self-assembly on surfaces is the possibility of exploiting the resulting structure to control surface properties, either directly through nanoscale pattern transfer, or through the controlled assembly of components for single molecule electronics. Over recent years the latter topic has attracted growing interest, and there have been several proposals for molecules with electronic properties analogous to conventional circuit elements such as diodes, switches, and wires.^{7,8} However, the realization

of any technology based on molecular components requires that such molecules may not only be synthesized but also arranged in a configuration where they interact to form a circuit. One approach to the problem of circuit assembly is to modify molecules of interest in order to promote intermolecular interactions which stabilize the required molecular arrangement.

In this paper we discuss a simple demonstrator of this principle. We show that the intermolecular interactions exhibited by naphthalene tetracarboxylic dianhydride (NTCDA) may be strongly modified through the incorporation of imide groups to form naphthalene tetracarboxylic diimide (NTCDI). Both of these molecules, NTCDA and NTCDI, have previously been investigated in relation to their application as active materials for molecular electronics.⁹ The presence of the imide groups results in the formation of extended chains stabilized by hydrogen bonding both in crystalline NTCDI and also following adsorption on Ag-terminated Si surfaces. We also demonstrate that self-assembled supramolecular structures can be subsequently modified, or processed, using the tip of a scanning tunneling microscope (STM).

NTCDI is synthesized through a reaction of NTCDA with ammonia (see Figure 1).⁷ Single crystals of NTCDI (typical dimensions 100 μm) were grown by thermal gradient sublimation [11] using a charge of ~ 40 mg heated in a stream of flowing Ar. Crystal growth from the gas phase was used to remove any solvent effects, often encountered in solution-based crystal growth, and to mimic the surface deposition methods used for subsequent STM studies. NTCDI is loaded into an ultrahigh vacuum system with a base pressure of 5

* Corresponding authors. E-mail: neil.champness@nottingham.ac.uk; peter.beton@nottingham.ac.uk.

[†] School of Physics & Astronomy.

[‡] School of Chemistry.

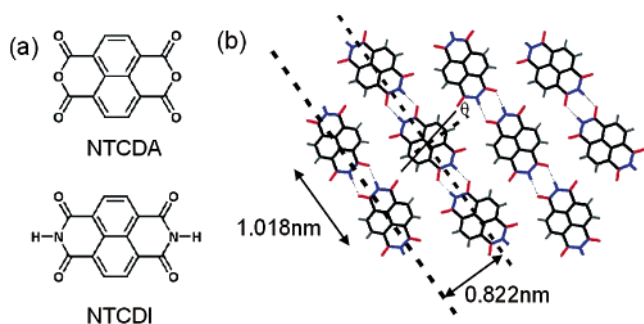


Figure 1. (a) Schematic diagrams showing the structure of naphthalene tetracarboxylic dianhydride (NTCDA) and naphthalene tetracarboxylic diimide (NTCDI). (b) Bulk crystal structure of NTCDI. Molecules are canted to the direction of the parallel rows within the crystal by an angle $\theta = \pm 13.9^\circ$.

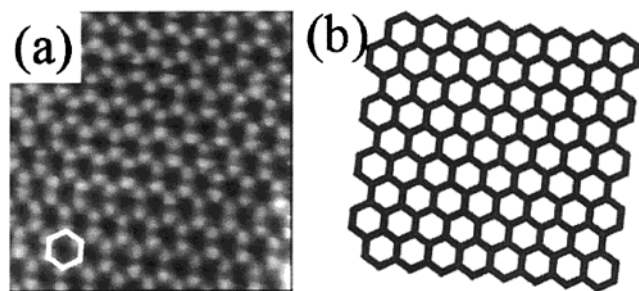


Figure 2. (a) STM image ($6 \times 6 \text{ nm}^2$, sample voltage +1 V, tunnel current 0.5 nA) of the $\text{Ag/Si}(111)\text{-}\sqrt{3} \times \sqrt{3}\text{R}30^\circ$ surface; (b) simplified schematic of the surface with vertices corresponding to positions of Ag trimers.

$\times 10^{-11}$ Torr and, following extended outgassing, sublimed onto a $\text{Ag/Si}(111)\text{-}\sqrt{3} \times \sqrt{3}\text{R}30^\circ$ surface. The source temperature was in the range 220–240 °C for which the deposition rate is typically ~ 10 monolayers/hour. Images of the surface are acquired using an STM operating at room temperature.

The $\text{Ag/Si}(111)\text{-}\sqrt{3} \times \sqrt{3}\text{R}30^\circ$ reconstruction is chosen as a substrate since molecules such as fullerenes^{12,13} and phthalocyanines¹⁴ have previously been studied on this surface and are found to diffuse freely and form islands in which the order is predominantly determined by intermolecular, as opposed to molecule–substrate, interactions. The energetic competitiveness of intermolecular interactions is essential for self-assembly to occur. This surface termination is prepared according to standard procedures which are described elsewhere.^{12–15} In Figure 2a an STM image of the $\text{Ag/Si}(111)\text{-}\sqrt{3} \times \sqrt{3}\text{R}30^\circ$ surface is shown. The atomic configuration of this surface has been studied extensively and is described by the honeycomb-chain-trimer model in which each surface Si atom is bonded to one Ag atom.¹⁵ Each bright topographic feature resolved in Figure 2a corresponds to a group of three Ag atoms, while the centers of the hexagons, which form a honeycomb network, correspond to a Si trimer.¹⁶ To simplify the subsequent discussion, we represent this surface by the schematic network shown in Figure 2b in which the vertices and centers of hexagons correspond, respectively, to Ag and Si trimers.

The crystal structure of NTCDI has been determined using single-crystal X-ray diffraction. (Crystal data for NTCDI

were measured as follows: $\text{C}_{14}\text{H}_6\text{N}_2\text{O}_4$, relative molecular mass $M_r = 266.21$, triclinic crystal system, space group $P\bar{1}$, $a = 7.6345(10)$, $b = 8.1774(11)$, $c = 8.9355(12)$ Å, $\alpha = 89.560(2)$, $\beta = 71.295(2)$, $\gamma = 80.065(2)^\circ$, $V = 519.8(2)$ Å³. Formula units per unit cell, $Z = 2$, density $D_c = 1.701$ g cm⁻³, conventional discrepancy $R = 4.37$; and weighted $wR2 = 9.83\%$, for 181 least-squares parameters and 2370 reflections, diffraction angle $2\theta_{\text{max}} = 57.4^\circ$.) Parallel planes of molecules are stacked with an interplane spacing of 0.311 nm, and the arrangement of molecules within a plane is shown in Figure 1b. Pairs of intermolecular N–H \cdots O hydrogen bonds are adopted at either end of the NTCDI molecules such that the molecules form rows in which the molecular axis (defined by the line connecting the centers of the aromatic rings forming the naphthalene core of the molecule) is canted at an angle $\theta = \pm 13.9^\circ$ with respect to the row axis. The canting maximizes the hydrogen bonding between the imide and carbonyl groups of neighboring molecules, and within a given plane the canting orientation alternates from row to row. The intermolecular spacing along the row is 1.018 nm, and the spacing between rows is 0.822 nm.

Images acquired following the adsorption of submonolayers of NTCDA and NTCDI on the $\text{Ag/Si}(111)\text{-}\sqrt{3} \times \sqrt{3}\text{R}30^\circ$ surface are shown in Figure 3. The deposition of NTCDA [Figure 3a] results in the formation of rather diffuse islands which are nucleated at step edges and defects in the Ag termination (note that Ag termination is ineffective at step edges and these regions, together with defects, have residual dangling bonds which act as preferential adsorption sites where island growth is nucleated). In addition there is some streaking in the images which is consistent with the presence of loosely bound adsorbates on the surface. This image should be contrasted with Figure 3b which is acquired following the deposition of ~ 0.5 monolayers of NTCDI. In this image there is no evidence of streaking and rows of molecules up to ~ 20 nm in length may be clearly resolved. Many, but not all, of these rows have been nucleated at step edges. It is clear from Figure 3b that the rows grow in one of three preferential directions which, as we show below, correspond to the principal axes of the $\text{Ag/Si}(111)\text{-}\sqrt{3} \times \sqrt{3}\text{R}30^\circ$ surface. The rows coexist on the surface with two-dimensional faceted islands. We stress that a comparison of Figures 3a and 3b confirms that the incorporation of the double hydrogen-bonding imide groups in NTCDI controls the supramolecular ordering on this surface.

Figure 3c shows a higher magnification image of an NTCDI chain. It is possible to resolve individual molecules within the chain and also submolecular detail. Images such as Figure 3c, in which the $\text{Ag/Si}(111)\text{-}\sqrt{3} \times \sqrt{3}\text{R}30^\circ$ surface may be resolved, show clearly that each row is aligned with one of the principal axes of the reconstructed surface and that the molecular spacing, d , is equal to $3a_0/2$, where $a_0 = 0.665$ nm is the lattice constant of the $\text{Ag/Si}(111)\text{-}\sqrt{3} \times \sqrt{3}\text{R}30^\circ$ surface. Thus $d = 0.998$ nm, within 0.02 nm of the spacing of molecules in the single-crystal structure (Figure 1). From such images it is also possible to determine the molecular adsorption sites as shown schematically in Figure

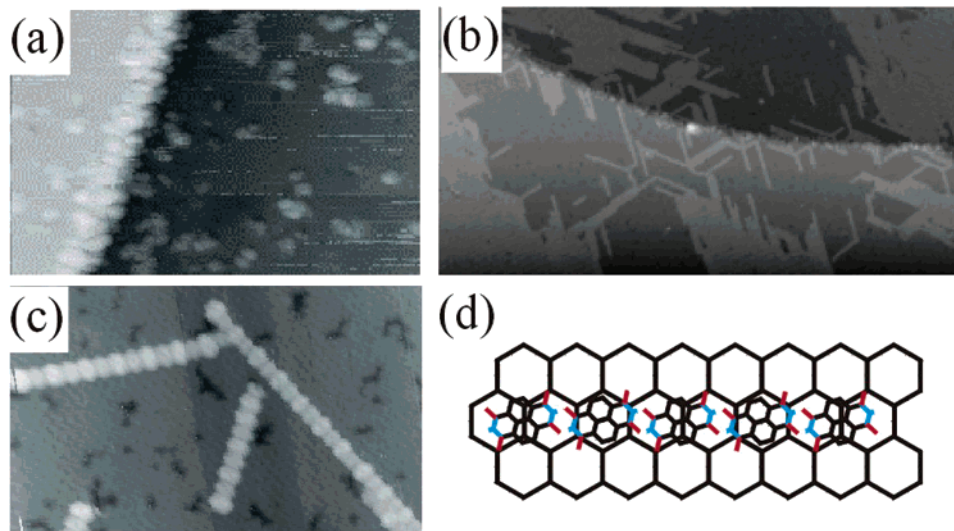


Figure 3. (a) $50 \times 65 \text{ nm}^2$ STM image (-3 V , -0.1 nA) showing $\sim 0.1 \text{ ML}$ NTCDA adsorbed on the $\text{Ag/Si(111)-}\sqrt{3} \times \sqrt{3} \text{R}30^\circ$ surface. Streaking in the image is characteristic of loosely bound molecules. (b) $95 \times 165 \text{ nm}^2$ STM image (-3 V , -0.05 nA) showing $\sim 0.5 \text{ ML}$ NTCDA adsorbed on the $\text{Ag/Si(111)-}\sqrt{3} \times \sqrt{3} \text{R}30^\circ$ surface (-1.2 V , -0.05 nA). Close packed islands and single-molecule-wide chains form spontaneously at room temperature. (c) $16 \times 26 \text{ nm}^2$ image (-1.2 V , -0.05 nA) showing high-resolution image of three molecular chains. (d) schematic diagram showing adsorption sites of molecules within a chain on the $\text{Ag/Si(111)-}\sqrt{3} \times \sqrt{3} \text{R}30^\circ$ surface.

3d. Note that, due to the half commensurability between d and a_o , alternate molecules along the chains are adsorbed above different sites on the surface. The canting angle may be estimated from our images as $\theta = 15 \pm 2^\circ$, extremely close to the value observed in the rows formed in bulk crystals. The close correspondence between the NTCDI rows observed on the $\text{Ag/Si(111)-}\sqrt{3} \times \sqrt{3} \text{R}30^\circ$ surface and the row motif observed in crystalline NTCDI confirms the importance of intermolecular H-bonding in surface ordering.

The adsorption of a closely related molecule, perylene-3,4,9,10-tetra-carboxylic-di-imide (PTCDI), in which similar H-bonding centers are present, has previously been investigated on hydrogen terminated Si(111).¹⁷ For PTCDI the growth of two-dimensional islands was observed. A key difference between our results and these earlier studies is the observation of isolated and extended *single* rows of molecules, and we believe that a balance between intermolecular and molecule–substrate interactions determines whether one- or two-dimensional growth occurs. In particular, high-resolution STM images of the two-dimensional islands which coexist with NTCDI rows reveal hexagonal order (see Figure 4). The separation between adjacent rows ($= 3\sqrt{3}a_o/4 = 0.864 \text{ nm}$) is greater by 0.04 nm than observed in bulk NTCDI. The larger row–row spacing exhibited on the $\text{Ag/Si(111)-}\sqrt{3} \times \sqrt{3} \text{R}30^\circ$ surface is presumably stabilized by molecule–substrate interactions at the expense of a reduction of the interactions between molecules in adjacent rows, resulting in the promotion of one-, rather than two-dimensional growth.

Bohringer et al.⁴ have shown previously that close packed clusters of molecules bound by noncovalent interactions may be positioned using the tip of an STM. Our results (see Figure 5) show that STM modification of rows of single molecules is also possible. We have found that by scanning with a reduced tip height (lower voltage and/or higher current than normally used for imaging) or through application of

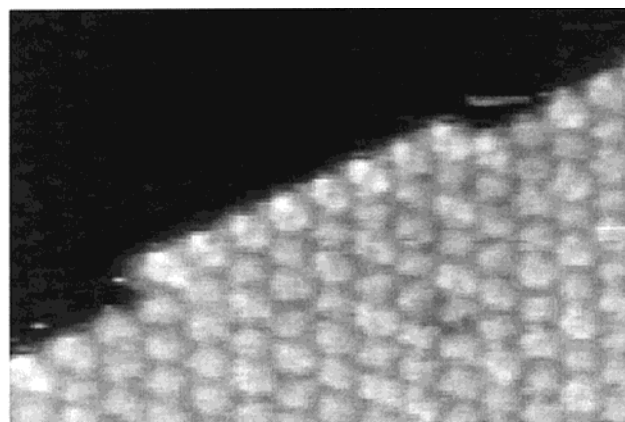


Figure 4. (a) $8 \times 16 \text{ nm}^2$ STM image (-3 V , -0.1 nA) showing hexagonal close packed island with major axes parallel to those of the $\text{Ag/Si(111)-}\sqrt{3} \times \sqrt{3} \text{R}30^\circ$ surface.

manipulation procedures previously used for room-temperature molecular manipulation,^{18–21} molecules may be removed or added to rows, and also that rows may be displaced across the surface. Only very limited control of these processes is possible at room temperature since single molecules may diffuse rapidly across the surface once they have been displaced from the ends of rows. Nevertheless, we have demonstrated (see Figure 5) that rows of molecules may be displaced as cohesive units. In Figure 5a three coincident rows may be resolved. After scanning this area these rows are disrupted and, of particular significance, a section of the rightmost row is displaced across the surface through two lattice constants (Figure 5b; the positions of the arrowed defects should be used for registry). Similarly a comparison of Figures 5c and 5d show a further example of such a displacement. In both cases an intervening scan performed with low positive sample bias ($+1.2 \text{ V}$) gives rise to the row manipulation. These results show that H-bonding

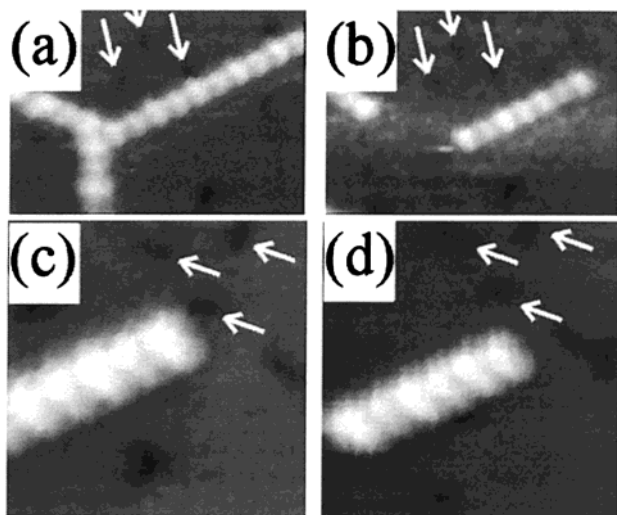


Figure 5. Examples of chain displacements: (a) and (b) 8×12 nm² STM image showing initial (a) and final (b) configuration of chains. (c) and (d) 8×8 nm² STM images showing another example of chain movement during scanning. Arrows mark defects for registry. All images were acquired using sample voltage -1.2 V, tunnel current 0.1 nA. In each case, intermediate scans with sample voltage $+1.2$ V, tunnel current 0.1 nA have resulted in the modification/displacement. In each case chains are moved by two surface lattice constants at an angle of 60° to chain axis.

is sufficiently strong to bind supramolecular rows together during displacement.

Our results are highly relevant to the growing interest in the electronic properties of single molecules. The results we have presented demonstrate that a rather minor change in the structure of a molecule may promote the formation of novel low dimensional supramolecular structures. It is clear that a similar approach, possibly in conjunction with STM modification for error correction, could be applied to the organization of molecular diodes, switches, and other components into complex arrangements corresponding, ultimately, to molecular circuits.

Acknowledgment. We are grateful to the UK Engineering and Physical Sciences Research Council for financial support.

Supporting Information Available: An X-ray crystallographic file, in CIF format, is available. This material is available free of charge via the Internet at <http://pubs.acs.org>.

References

- (1) Lehn, J.-M. *Supramolecular Chemistry*; VCH: Weinheim, Germany, 1995.
- (2) Barth, J. V.; Weckesser, J.; Cai, C.; Gunter, P.; Burgi, L.; Jeandupeux O.; Kern, K. *Angew. Chem., Int. Ed.* **2000**, *39*, 1230.
- (3) Yokoyama, T.; Yokoyama, S.; Kamikado, T.; Okuno, Y.; Mashiko, S. *Nature* **2001**, *413*, 619.
- (4) Bohringer, M.; Morgenstern, K.; Schneider, W.-D.; Berndt, R. *Angew. Chem., Int. Ed.* **1999**, *38*, 821.
- (5) Bohringer, M.; Morgenstern, K.; Schneider, W.-D.; Berndt, R.; Mauri, F.; de Vita, A.; Car, R. *Phys. Rev. Lett.* **1999**, *83*, 324.
- (6) Griessl, S.; Lackinger, M.; Edelwirth, M.; Hietschold, M.; Heckl, W. M. *Single Mol.* **2002**, *3*, 25.
- (7) Aviram, A.; Ratner, M. *Chem. Phys. Lett.* **1974**, *29*, 277.
- (8) Joachim, C.; Gimzewski, J. K.; Aviram, A. *Nature* **2000**, *408*, 541.
- (9) (a) Laquindanum, J. G.; Katz, H. E.; Dodabalapur, A.; Lovinger, A. *J. J. Am. Chem. Soc.* **1996**, *118*, 11331. (b) Forrest, S. R. *Chem. Rev.* **1997**, *97*, 1793, and references therein.
- (10) Sotiriou-Leventis, C.; Mao, Z. *J. Heterocyclic Chem.* **2000**, *37*, 1665.
- (11) Laudise, R. A.; Kloc, C.; Simpkins, P. G.; Siegrist, T. *J. Cryst. Growth* **1998**, *187*, 449.
- (12) Upward, M. D.; Moriarty, P.; Beton, P. H. *Phys. Rev. B* **1997**, *56*, R1704.
- (13) Butcher, M. J.; Nolan, J. W.; Hunt, M. R. C.; Beton, P. H.; Dunsch, L.; Kuran, P.; Georgi, P.; Dennis, T. J. S. *Phys. Rev. B* **2001**, *64*, 195401.
- (14) Upward, M. D.; Beton, P. H.; Moriarty, P. *Surf. Sci.* **1999**, *441*, 21.
- (15) (a) Takahashi, T.; Nakatani, S.; Okamoto, N.; Ichikawa, T.; Kikuta, S. *Surf. Sci.* **1991**, *242*, 54. (b) Katayama, M.; Williams, R. S.; Kato, M.; Nomura, E.; Aono, M. *Phys. Rev. Lett.* **1991**, *66*, 2762.
- (16) Wan, K. J.; Lin, X. F.; Nogami, J. *Phys. Rev. Lett.* **1993**, *47*, 13700.
- (17) Uder, B.; Ludwig, C.; Petersen, J.; Gompf, B.; Eisenmenger, W. Z. *Phys.* **1995**, *B97*, 389.
- (18) Moriarty, P.; Ma, Y.-R.; Upward, M. D.; Beton, P. H. *Surf. Sci.* **1998**, *407*, 27.
- (19) Humphry, M. J.; Chettle, R.; Moriarty, P.; Upward, M. D.; Beton, P. H. *Rev. Sci. Instrum.* **2000**, *71*, 1698.
- (20) Beton, P. H.; Dunn, A. W.; Moriarty, P. *Appl. Phys. Lett.* **1995**, *67*, 1075.
- (21) Jung, T. A.; Schlitter, R. R.; Gimzewski, J. K.; Tang, H.; Joachim, C. *Science* **1996**, *271*, 181.

NL025821B